Review Article

Positron emission tomography and magnetic resonance imaging in primary central nervous system lymphoma—a narrative review

Simone Krebs[1], Julia G. Barasch[2], Robert J. Young[3,4], Christian Grommes[4,5], Heiko Schöder[1]

[1]Molecular Imaging and Therapy Service, Department of Radiology, Memorial Sloan Kettering Cancer Center, New York, NY, USA; [2]Vagelos College of Physicians and Surgeons, Columbia University, New York, NY, USA; [3]Neuroradiology Service, Department of Radiology, Memorial Sloan Kettering Cancer Center, New York, NY, USA; [4]Brain Tumor Center, Memorial Sloan Kettering Cancer Center, New York, NY, USA; [5]Department of Neurology, Memorial Sloan Kettering Cancer Center, New York, NY, USA

Contributions: (I) Conception and design: All authors; (II) Administrative support: None; (III) Provision of study materials or patients: None; (IV) Collection and assembly of data: All authors; (V) Data analysis and interpretation: None, (VI) Manuscript writing: All authors; (VII) Final approval of manuscript: All authors.

Correspondence to: Heiko Schöder. 1275 York Ave, Box 77, New York, NY 10065, USA. Email: schoderh@mskcc.org.

Abstract: This review addresses the challenges of primary central nervous system (CNS) lymphoma diagnosis, assessment of treatment response, and detection of recurrence. Primary CNS lymphoma is a rare form of extra-nodal non-Hodgkin lymphoma that can involve brain, spinal cord, leptomeninges, and eyes. Primary CNS lymphoma lesions are most commonly confined to the white matter or deep cerebral structures such as basal ganglia and deep periventricular regions. Contrast-enhanced magnetic resonance imaging (MRI) is the standard diagnostic modality employed by neuro-oncologists. MRI often shows common morphological features such as a single or multiple uniformly well-enhancing lesions without necrosis but with moderate surrounding edema. Other brain tumors or inflammatory processes can show similar radiological patterns, making differential diagnosis difficult. [18F]-fluorodeoxyglucose (FDG) positron emission tomography (PET) has selected utility in cerebral lymphoma, especially in diagnosis. Primary CNS lymphoma can sometimes present with atypical findings on MRI and FDG PET, such as disseminated disease, non-enhancing or ring-like enhancing lesions. The complementary strengths of PET and MRI have led to the development of combined PET-MR systems, which in some cases may improve lesion characterization and detection. By highlighting active developments in this field, including advanced MRI sequences, novel radiotracers, and potential imaging biomarkers, we aim to spur interest in sophisticated imaging approaches.

Keywords: Primary central nervous system lymphoma (primary CNS lymphoma); positron emission tomography (PET); magnetic resonance imaging (MRI); imaging

Received: 16 December 2020; Accepted: 10 March 2021; Published: 30 June 2021.
doi: 10.21037/aol-20-52
View this article at: http://dx.doi.org/10.21037/aol-20-52

Introduction

Epidemiology

Primary central nervous system (CNS) lymphoma is a rare and aggressive subtype of extra-nodal non-Hodgkin lymphoma confined to the brain, spinal cord, leptomeninges, or eyes. With an incidence of 0.44 per 100,000, primary CNS lymphoma accounts for approximately 2% of all primary CNS tumors in the US (1). Diffuse large B-cell lymphoma (DLBCL) is the most common histological subtype (2) (approximately 90%) of primary CNS lymphomas; the other subtypes are Burkitt lymphoma, low-grade lymphoma, and T-cell lymphoma (3). The median age at disease presentation is 65 years, with an increasing incidence in the elderly.

Immunodeficiency constitutes an important risk factor

for the development of primary CNS lymphoma (4). This includes human immunodeficiency virus (HIV) infection as well as congenital immune deficiency syndromes (e.g., ataxia-telangiectasia, severe combined and common variable immunodeficiency syndromes (incidence up to 4%), and more common acquired immune suppression states (e.g., patients with cancer and transplant recipients). Patients receiving the highest levels of suppression, such as lung and liver transplant recipients, have the highest risk of developing primary CNS lymphoma, usually from B-lymphocyte infection by the Epstein-Barr virus (EBV) (5-7). Following kidney, heart, or lung transplantation, the frequency of post-transplant lymphoproliferative disorders localized in the CNS is estimated to be 1–7%. Infections with EBV or iatrogenic T-lymphocyte dysfunctions play a key role in the pathogenesis of these processes. However, primary CNS lymphoma developing in immunocompetent patients is not associated with EBV (3), and its incidence in these patients has continued to rise over the past three decades for unexplained reasons (8). Interestingly, in patients with AIDS, the incidence of primary CNS lymphoma seems to be decreasing due to successful antiretroviral therapies (9).

Histopathology

Gene expression profiling has identified three molecular subgroups of non-CNS DLBCL, including the germinal center B-cell like, activated B-cell like, and type 3 subgroups (10). The vast majority of primary CNS lymphomas are DLBCL, belonging to the activated B-cell like subtype, and have an activated B-cell immunophenotype resembling exit of B-cells from the germinal center (2). Genomic sequencing has identified alterations in genes within the B-cell receptor signaling axis at increased frequencies. Two such genes, *MYD88* and *CD79B*, implicate the involvement of primary CNS lymphoma.

Treatment

The treatment for primary CNS lymphoma has continuously evolved; currently, no optimal first-line chemotherapy exists. Methotrexate (MTX)-based chemotherapy has become the standard of care, but most patients relapse and the 5-year survival rate remains inferior to that of patients with DLBCL outside the nervous system (11-13). Moreover, the prognosis of elderly patients and patients with relapsed or refractory disease remains poor (14,15). Although new therapeutic regimens have improved survival (16-18), the management of this disease remains challenging to the neuro-oncology community.

Clinical presentation and diagnosis

Most patients present with focal neurologic deficits related to the involved CNS compartment. However, about 43% of patients exhibit behavioral or neurocognitive changes (such as headache, confusion, nausea, vomiting, or seizures) that are non-specific and possibly related to the mass effect, resulting in delayed diagnosis (19).

Most primary CNS lymphoma lesions are located in the periventricular region and involve the white matter of the centrum semiovale or corona radiata, or in the corpus callosum, basal ganglia, or, rarely, spinal cord. Primary CNS lymphomas can occur with multifocal lesions; leptomeningeal involvement is detected in 15–20% of cases (20).

The diagnosis of primary CNS lymphoma requires histopathological evaluation of tissue samples or cerebrospinal fluid (CSF). In addition, immunophenotype and genetic studies are often performed. Detection of lymphoid cells in the CSF can eliminate the need for biopsy (21). However, characteristic cells are only detected in one-third of cases, and a "negative" CSF examination does not rule out primary CNS lymphoma. Recently, analysis of microRNA (non-coding RNA molecules, regulating other gene expressions) from CSF has shown potential diagnostic utility. In particular, miR-21, mir-19b, and miR-92a are reported to have 96.7% specificity for primary CNS lymphoma (22,23). Several clinical, laboratory, and imaging studies are necessary for proper staging of the disease. These include physical examination, ophthalmic evaluation with a slit-lamp examination, analysis of serum lactate dehydrogenase (LDH) levels, HIV testing, contrast-enhanced brain magnetic resonance imaging (MRI), and lumbar puncture (LP). In patients who cannot undergo LP or in those with evidence of spinal cord dysfunction, contrast-enhanced MRI of the entire spine should be considered (24). To identify potential lymphoma lesions outside the CNS (which would change the diagnosis to secondary CNS lymphoma and lead to different treatment planning (25-27), complete systemic staging including computed tomography (CT) scan of the chest, abdomen, and pelvis as well as bone marrow biopsy with aspirate are recommended. Testicular ultrasonography studies should also be considered in men.

Performance of a body fluorodeoxyglucose (FDG)

positron emission tomography (PET)/CT has been recommended by several centers inside and outside the US, including our group (19,28-31); however, in the past, it was not included in guidelines by the International Primary CNS Lymphoma Collaborative Group (IPCG). For systemic staging, a whole-body FDG PET may be preferential to and obviate whole-body CT scan and testicular sonography.

This narrative review addresses the role of imaging, including challenges of primary CNS lymphoma diagnosis and treatment monitoring, and outlines its potential for prognostic applications. We present the following article in accordance with the Narrative Review reporting checklist (available at http://dx.doi.org/10.21037/aol-20-52).

MRI

Gadolinium-enhanced brain MRI is the modality of choice for the assessment of primary CNS lymphoma. A presumptive diagnosis may be made based on the imaging appearance and tumor response to corticosteroids. However, since other processes including multiple sclerosis, sarcoidosis, and occasional gliomas may show similar imaging features and demonstrate initial response to corticosteroids, tissue diagnosis remains essential. Early and accurate prediction and diagnosis of primary CNS lymphoma is critical, as its management differs from that of many other CNS tumors (6). Corticosteroids are empirically given to many patients with newly diagnosed brain tumors, particularly symptomatic patients, in order to reduce swelling and mass effect. However, since histopathology for primary CNS lymphoma in the setting of corticosteroid therapy is often negative, patients with possible disease should not receive corticosteroid therapy before sampling. In addition, since gross total resection has not been shown to improve survival, most patients with primary CNS lymphoma require only biopsy for diagnosis. In patients with contraindications to MRI, contrast-enhanced CT scans may suffice. Although mostly used for screening, non-contrast CT in conjunction with MRI has been reported as useful to differentiate primary CNS lymphoma from similar entities (32).

The European Association of Neuro-Oncology (EANO) guidelines recommend brain MRI using T2-weighted/fluid-attenuated inversion recovery (T2/FLAIR) and T1-weighted sequences pre-contrast and post-contrast injection for diagnosis and follow-up (33). Studies have suggested that post-contrast T2/FLAIR images are more sensitive for detecting disease, with the combination of T1- and T2-weighting to suppress the signal from bulk fluid helping to increase lesion conspicuity particularly for leptomeningeal disease near the cortex or subependymal disease along the ventricles (34,35). The recommendations specify T2/FLAIR acquisition after contrast injection and prior to post-contrast T1-weighted images. Since the EANO does not specify MRI acquisition parameters such as slice thickness, time-to-echo, and time-to-repetition, we encourage sites to follow the consensus recommendation standardized brain tumor imaging protocol when possible (36). Those standardized brain tumor imaging protocols were not developed explicitly for primary CNS lymphoma, however, and notably recommend only pre-contrast T2/FLAIR that differs from the EANO post-contrast T2/FLAIR recommendations. Since post-contrast T2/FLAIR images are not standard at many institutions, and therefore possibly less familiar to many radiologists when searching for pathology and/or dismissing artifacts, we suggest that sites establish and follow their own local best practices. Diffusion, dynamic susceptibility contrast (DSC), proton spectroscopy MRI, and FDG PET have also been recognized as useful adjuncts for differential diagnosis and management, although they may have limited specificity and their application will also depend on local expertise.

Advanced MRI

In contrast to conventional MRI, which evaluates anatomy, advanced MRI enables characterization of tumor biology and physiology. These tools include diffusion, perfusion, and spectroscopy imaging.

Diffusion

Diffusion-weighted imaging (DWI) measures the motion of water molecules in tissue. Diffusion restriction occurs when intact cells impede otherwise Brownian or random water motion; diffusion restriction, while complex, is correlated with cellularity (37). Primary CNS lymphoma causes highly cellular tumors that typically present with hyperintense signal on b-1,000 DWI and hypointense signal on calculated apparent diffusion coefficient (ADC) maps. Pretreatment ADC values can be helpful in establishing diagnosis and predicting prognosis, with low ADC values correlating with shorter progression-free (PFS) and overall (OS) survival times (6,37). DWI may also inform treatment decisions. Patients with greater changes in ADC values after

high-dose MTX-based chemotherapy show better clinical outcomes (29,37).

Diffusion tensor imaging (DTI) enables more sensitive detection of white matter microstructure changes. The primary metric, fractional anisotropy, is a unitless measure of diffusion anisotropy or directionality. Decreased fractional anisotropy in primary CNS lymphoma is thought to reflect the decreased extracellular space caused by tumor growth (38); however, this finding is non-specific and also observed in most other disease entities.

Perfusion

Perfusion imaging enables the quantitative evaluation of tumor microvasculature and has been correlated with microvascular density at histopathology as well as catheter angiography. The most popular perfusion techniques are DSC T2* imaging and dynamic contrast-enhanced (DCE) T1 imaging, which utilize exogenous gadolinium contrast injection, and arterial spin labeling (ASL), which utilizes flowing blood as endogenous contrast. Although DSC perfusion is more rapid and more widely applied, it is vulnerable to degradation by susceptibility artifacts from bone, calcification, and hemorrhage. DCE perfusion has higher spatial resolution but more complex pharmacokinetic modeling and is sensitive to arterial input function selection.

Primary CNS lymphoma demonstrates primarily angiocentric growth (6) and lacks florid neoangiogenesis, resulting in near normal or only slightly elevated perfusion values that are much lower than those found in high-grade gliomas (HGGs). These perfusion changes are attributable in part to the disruption of the blood-brain barrier (39), although any changes are vulnerable to the efficiency of T1 and T2* leakage correction methods (40). Pretreatment low relative cerebral blood volume (rCBV, derived from DSC perfusion) and low plasma volume (VP, derived from DCE perfusion) imply poor tumor vascularity and predict worse PFS and OS (41-43), presumably due to poor penetration of chemotherapy into the tumor. Similarly, low-contrast volume transfer coefficient Ktrans (also derived from DCE perfusion, a measure of leakiness or permeability including blood-brain barrier disruption) is also correlated with worse survival (42). In addition, the combination of low perfusion and low ADC portends a particularly poor prognosis (43).

Spectroscopy

MR spectroscopy enables the noninvasive quantification of biochemical information from tissues. The most commonly used nuclei are protons (measured as hydrogen particles). Spectroscopy of primary CNS lymphoma typically demonstrates a nonspecific tumor spectrum with increased choline (a cell membrane marker) due to high cell membrane turnover. There are also very high lipid/lactate peaks (anaerobic glycolysis marker) due to macrophage infiltration, and nonspecific low N-acetylaspartate (NAA, a neuronal marker). This technique, in conjunction with other imaging techniques, may help with differential diagnosis of primary CNS lymphoma but cannot alone diagnose or differentiate the disease from other similar tumors (44).

Imaging patterns

Presentation in immunocompetent patients

Classic presentation

The most common presentation of primary CNS lymphoma is a solitary lesion in adults (approximately 70% of cases) that is hyperdense on CT, hypointense to isointense on T2-weighted images, and homogeneously enhancing [primary CNS lymphoma invades the perivascular spaces and blood vessel walls, causing damage to the blood-brain barrier (41)]. The dense cellularity manifests with diffusion restriction on DWI with hyperintense signal on b-1,000 images and corresponding hypointense signal on calculated ADC maps (29). The enhancing lesion is typically surrounded by moderate hypodense on CT or T2-hyperintense perilesional edema, although there is classically little mass effect relative to size.

Most lesions occur in the supratentorial brain and involve the periventricular white matter, deep gray nuclei, corpus callosum, or meningeal margins (*Figures 1-3*) (45). The tumors are hyperdense on CT and hypointense on T2-weighted MRI due to innate hypercellularity with high nucleus-to-cytoplasmic ratios. Characteristically, even larger lesions exert little if any mass effect; subcortical lesions often wrap around the cortex in a crescentic shape instead of altering the morphology. Edema is common in primary CNS lymphoma, as in many other brain tumors (6). Hemorrhage, calcification, heterogeneous enhancement, and cystic/necrotic changes are rarely found at presentation in immunocompetent patients.

Less common presentations

A third or more of patients will present with multiple lesions at diagnosis (6,45). Less common locations include the cerebellum and brainstem, although primary CNS

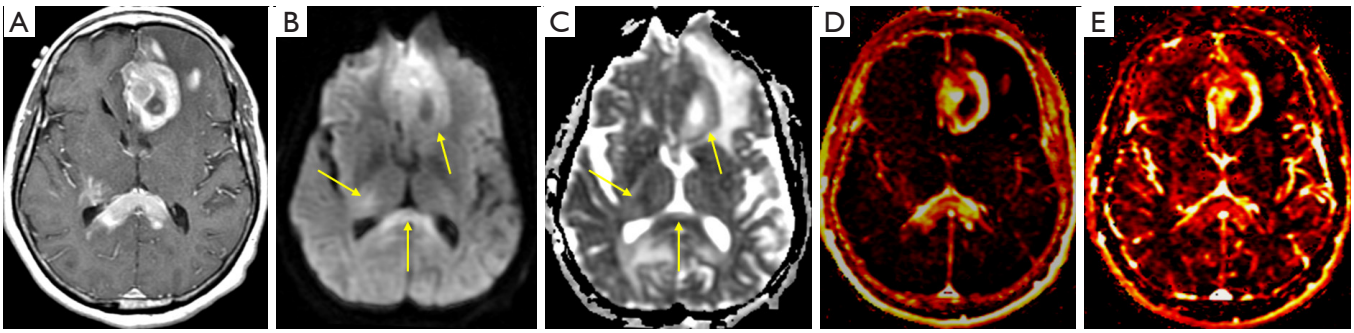

Figure 1 A 72-year-old female with increasing forgetfulness, confusion, and irritability. Axial contrast T1-weighted image (A) demonstrates multiple large homogeneously and heterogeneously enhancing lesions in the anterior and posterior corpus callosum and frontal lobes and right basal ganglia and thalamus (arrows), with relatively little mass effect. The lesions demonstrate diffusion restriction with hyperintense signal on b-1,000 (B) and hypointense signal on ADC (C) images. Perfusion reveals heterogeneously increased Ktrans (D) and slightly increased plasma volume (E), particularly the lesion in the splenium of the corpus callosum. ADC, apparent diffusion coefficient.

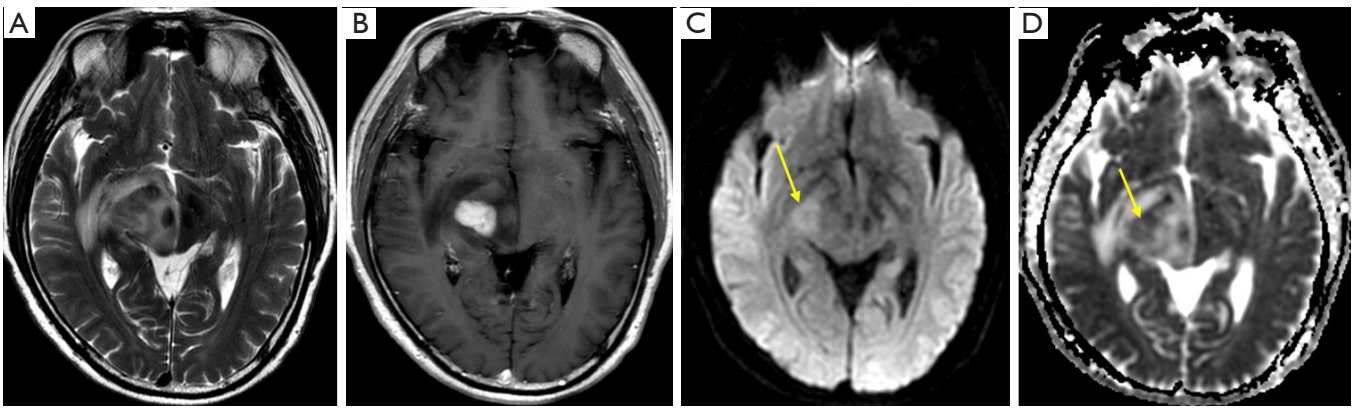

Figure 2 A 65-year-old man with gait instability and headache. Axial T2-weighted (A) and contrast T1-weighted (B) images demonstrate a heterogeneously hypointense enhancing lesion in the right midbrain, and moderate adjacent edema with mild compression of the third ventricle. The lesion is diffusion restricted (arrows) with hyperintense signal on b-1,000 diffusion-weighted image (C) and hypointense signal on ADC map (D). ADC, apparent diffusion coefficient.

lymphoma may occur almost anywhere in the CNS. In addition to parenchymal disease, the disease may present with primary involvement of the perivascular spaces, leptomeninges, pituitary infundibulum, dura, eye, spinal cord, and nerve roots (neurolymphomatosis). Although usually intense and homogeneous, the enhancement may variably be mild, have a peripheral ring shape, or be heterogeneous with areas of cystic/necrotic change. Rare forms may present with only T2-hyperintense lesions with variable diffusion restriction and no enhancement.

Primary leptomeningeal lymphoma

Primary leptomeningeal lymphoma is a rare form of primary CNS lymphoma limited to the leptomeninges, manifesting with enhancing leptomeningeal lesions on contrast T1-weighted images; for instance, along the surfaces of the brain, brainstem, cranial nerves, spinal cord, and/or cauda equina nerve roots. Of note, MRI abnormalities are found in only 74% of patients, while the CSF is always abnormal (46). Hydrocephalus resulting from disruption of CSF resorption due to tumor infiltration of the subarachnoid spaces is found in only 9%. Leptomeningeal spread occurs in 11–16% of patients with primary CNS lymphoma (20,47,48).

The pattern of enhancing leptomeningeal lesions is indistinguishable from other diseases that may affect the subarachnoid space. These include metastases (from primary brain cancers, systemic cancers, lymphoma, or

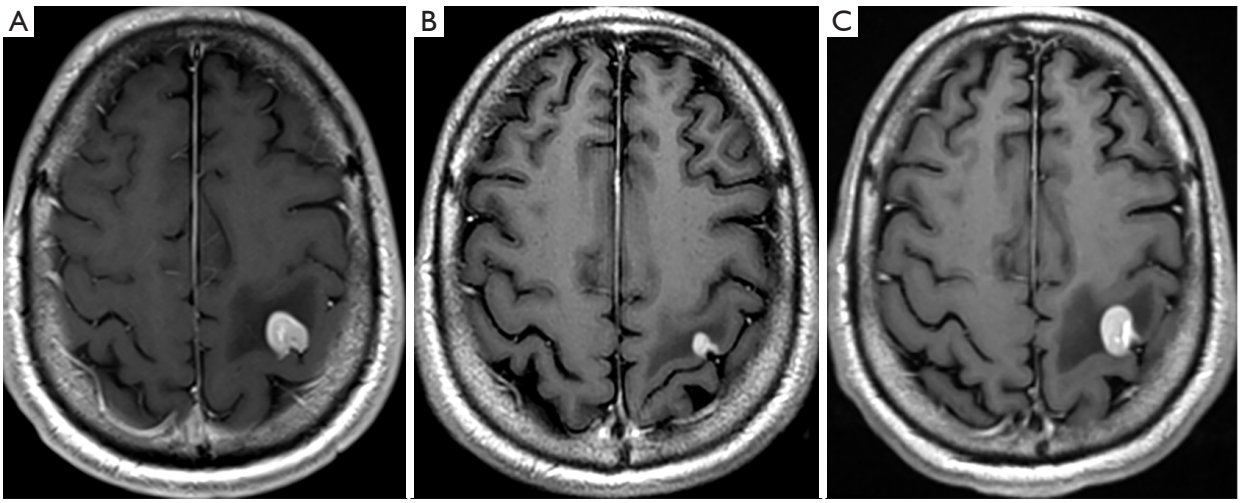

Figure 3 A 56-year-old man with right hand clumsiness. Axial contrast T1-weighted images: at presentation (A), there is a well circumscribed homogeneously enhancing lesion in the left precentral (motor) gyrus and mild adjacent hypointense edema. The patient received steroids with symptom improvement. Three weeks later, repeat scan (B) showed dramatic decrease in size of the enhancing lesion. The steroids were discontinued and biopsy postponed for another two weeks (C), when the lesion had increased again and pathology confirmed diffuse large B-cell lymphoma.

leukemia), meningitis, and granulomatous disease (e.g., neuro-sarcoidosis).

Differential diagnosis of primary CNS lymphoma in immunocompetent patients

The differential diagnosis includes brain tumors such as HGGs, tumefactive demyelinating lesions (TDLs), and infectious granulomatous diseases (29). A combination of imaging techniques, including MRI, may be helpful to differentiate between these entities. Specificity is improved by incorporating clinical scenarios and CSF analysis. Biopsy or resection remains necessary in uncertain cases. When primary CNS lymphoma is a possibility, corticosteroids should be withheld as they may confound the diagnosis (*Figure 3*).

In contrast to primary CNS lymphoma, HGG displays heterogeneous enhancement with cystic/necrotic changes, although there is considerable overlap in presentation on conventional MRI. Both entities may be centered in the corpus callosum in a butterfly pattern, but primary CNS lymphoma more frequently infiltrates the optic tracts and the basal ganglia, while HGG is typically found in the cerebral cortex. On DWI, ADC values are useful in differentiation (primary CNS lymphomas have lower ADC because of higher cellularity than HGG), especially when used in conjunction with conventional MRI (29,49,50). Ideally, imaging is performed with slice thickness <3 mm to reduce heterogeneity and artifacts (50). The decrease in fractional anisotropy in primary CNS lymphoma is also more marked than the decrease in glioblastoma (GBM), although this DTI metric has been described as less specific and less accurate than changes in ADC (38). On perfusion imaging, angiocentric growth and lower microvascular density of primary CNS lymphoma result in relatively normal or slight increases in perfusion. In contrast, the neo-angiogenesis and higher microvascular density in GBM causes markedly increased perfusion (6). Two recent meta-analyses found high accuracy for perfusion imaging to distinguish between primary CNS lymphoma and HGGs with areas under the curve (AUCs) of 0.94–0.96 (51,52). DSC was the most sensitive technique, and ASL the most specific technique (51) although other authors have suggested a dual DCE + DSC perfusion approach (53). Measurements in the peritumoral abnormality may also reveal increased perfusion in HGGs that is absent in primary CNS lymphoma (54). Overall, perfusion studies demonstrate high accuracy in differentiating between HGGs and primary CNS lymphoma (51) (see *Table 1* for further details).

(I) Demyelinating disease

Demyelinating disease is categorized as TDLs when the clinical presentation and imaging findings cannot distinguish lesions from neoplasm. Clinically, patients

Table 1 Typical findings in primary CNS lymphoma and common differential possibilities. Numbers in parentheses indicate representative values in our experience and from the literature, although the considerable heterogeneity in methodology including acquisition, postprocessing, and measurements limits straightforward application (39,42,49,55-62)

Diagnosis	Diffusion	Perfusion		MR spectroscopy		
	ADC (10^{-6} mm^2/s)	rCBV (DSC)	VP (DCE)	Cho/Cr	Lac/Cr	Lip/Cr
Primary CNS lymphoma	Very low (510–900)	Near normal or slightly high (0.7–1.2)	Near normal or slightly high (0.5–2.4)	Very high (2.6–4.3)	Very high (2.5–11.8)	Very high (3.4–26.7)
Glioblastoma	Variable (700–1300)	High (1.8–3.6)	High (3.9–6.9)	Slightly high (1.8–2.5)	Variable (0.4–4.5)	Variable (0.4–23.5)
Anaplastic astrocytoma	Variable (700–1300)	High (1.8–3.4)	High (2.4–4.3)	Slightly high (1.8–2.6)	Low (0.8–1.3)	Low (0.9–1.4)
Metastasis	Variable (600–1500)	High (1.8–3.1)	High (3.4–6.8)	Slightly high (0.4–1.6)	Low (0.2–0.4)	High (2.8–6.4)

ADC, apparent diffusion coefficient; rCBV, relative cerebral blood volume; DSC, dynamic susceptibility contrast; VP, plasma volume; DCE, dynamic contrast enhanced; Cho/Cr, choline/creatine; Lip/Cr, lipid/creatine; Lac/Cr, lactate/creatine.

with primary CNS lymphoma are usually older, do not show improvement in symptoms following demyelination disease treatment, and do not have spinal cord involvement. TDLs are usually >2 cm (63). When present, mass effect and heterogeneous enhancement may help differentiate these lesions from primary CNS lymphoma. In rare cases, primary CNS lymphoma may be preceded by sentinel demyelination, which can mimic multiple sclerosis or acute disseminated encephalomyelitis (ADEM). On DWI, TDLs have variable, heterogeneous ADC values that depend on the temporal evolution of the demyelination (29). Acute TDLs can demonstrate marked diffusion restriction, even prior to enhancement, which classically occur at the lesion periphery along the leading edge of active demyelination. The diffusion restriction manifest by low ADC is postulated to be due to high cellularity, intramyelinic edema, and/or cytotoxic edema (64). The centers typically demonstrate facilitated diffusion with high ADC values related to myelin destruction and edema. These findings contrast with the homogeneous diffusion restriction in primary CNS lymphoma, where hypercellularity is the predominant contributor to the low ADC. Finally, on spectroscopy, increased glutamate and glutamine peaks in demyelinating lesions may be helpful for differentiation (whereas many tumors show increased choline and lactate peaks) (44).

(II) CNS metastases from extracranial primary tumors

CNS metastases from extracranial primary tumors are typically located at the gray-white matter junctions and show either homogeneous or heterogeneous enhancement with abundant surrounding edema (29,65). Primary CNS lymphoma lesions usually cause less edema and less mass effect than metastatic lesions of similar size (6). On diffusion imaging, metastases may show diffusion restriction in the enhancing solid components but diffusion facilitation in cystic and/or necrotic components. Comparatively, primary CNS lymphoma shows homogeneous diffusion restriction and significantly lower ADC values than metastases (29,66). Moreover, metastases often cause neovascularization as they expand (67), leading to markedly increased perfusion, similar to HGGs. In contrast, primary CNS lymphoma usually has near normal perfusion (44,66).

Presentation in immunodeficient patients

Immunodeficient patients almost always present with multiple lesions that demonstrate heterogeneous enhancement and cystic/necrotic changes. HIV-associated primary CNS lymphoma often presents with multiple supratentorial lesions in the periventricular regions and contain hemorrhage.

An important differential diagnosis in immunodeficient patients is progressive multifocal leukoencephalopathy (PML). This is caused by the activation of latent John Cunningham (JC) virus in HIV and other immunodeficient patients. Demyelination occurs due to the destruction of the myelin-producing oligodendrocytes. Scans typically demonstrate confluent bilateral asymmetric supratentorial white matter lesions with absent or little mass effect and enhancement. The demyelination characteristically extends to the subcortical U-fibers, which occurs less commonly in multiple sclerosis, and also involves the gray matter in late

Table 2 Response criteria for primary central nervous system lymphoma according to IPCG

Response	Brain imaging	Corticosteroid dose	Eye examination	CSF cytology
CR	No contrast enhancement	None	Normal	Negative
Cru	No contrast enhancement	Any	Normal	Negative
	Minimal abnormality	Any	Minor RPE abnormality	Negative
PR	50% decrease in enhancing tumor	Irrelevant	Minor RPE abnormality or normal	Negative
	No contrast enhancement	Irrelevant	Decrease in vitreous cells or retinal infiltrate	Persistent or suspicious
PD	25% increase in lesion	Irrelevant	Recurrent or new ocular disease	Recurrent or positive
	Any new site of disease: CNS or systemic			

CR, complete response; Cru, unconfirmed complete response; RPE, retinal pigment epithelium; PR, partial response; PD, progressive disease.

stages. The classic PML presentation with non-enhancing white matter lesions is different from the classic primary CNS lymphoma presentation with diffusion restricted enhancing lesions; however, PML remains an important diagnostic consideration in immunodeficient patients and may mimic the less common chameleon presentation of primary CNS lymphoma non-enhancing white matter lesions at diagnosis or recurrence (68). Effective treatment of HIV may also result in worsening imaging abnormalities due to PML-related immune reconstitution inflammatory syndrome (PML-IRIS). These PML-IRIS scans usually present with patchy enhancing lesions. Given the wide spectrum of possible presentations of primary CNS lymphoma, these too may occasionally present a diagnostic dilemma.

Cerebral toxoplasmosis is the most classic infection in patients with HIV and other immunodeficient conditions such as transplant patients and rheumatoid arthritis or multiple sclerosis patients requiring immunosuppression. Toxoplasmosis is most frequently found in the basal ganglia, cerebral cortex, or brainstem, in contrast to primary CNS lymphoma, which is usually periventricular and may have subependymal or leptomeningeal spread. An "eccentric target sign" may be seen on contrast T1 images (29). Other unusual infections include tuberculosis and fungal diseases such as Aspergillosis and Candidiasis, which may present with brain, meningeal, and/or leptomeningeal lesions.

Response criteria

In 2005, the IPCG established guidelines to standardize the baseline evaluation and response criteria of patients with primary CNS lymphoma (69). They established contrast-enhanced MRI scans as the standard of care for imaging, although both unidimensional and bidimensional measurements were allowed akin to the RECIST 1.1 and Response Assessment in Neuro-Oncology (RANO) criteria (70,71). Response is determined based on evaluation of a patient's enhancement patterns on neuroimaging, ophthalmologic exam, CSF cytology, and dependence on corticosteroids. These criteria help guide the appropriate triaging and grouping of primary CNS lymphoma patients, predict prognosis, and standardize imaging intervals and measurement techniques. Thereby they enable more direct and accurate comparisons of the efficacy of different primary CNS lymphoma treatments and clinical trials. *Table 2* summarizes the response criteria established by the IPCG (69). There are several distinct limitations to the IPCG criteria, despite its near ubiquitous use enabling comparison of modern trials to historical trials. The primary clinical limitation, which is common to most standardized response criteria, is the imprecision in characterizing individual patients who may have highly variable presentations and clinical trajectories. The IPCG criteria do not formally incorporate any advanced MRI or PET imaging techniques. Changes in enhancing lesion size are known to lag changes in tumor physiology detectable by advanced imaging. In clinical trials and daily practice, we incorporate our institutional standard of care advanced imaging to confirm possible progressive disease (PD) when increases in size occur.

Surveillance after treatment

At least one-half of patients who achieve complete response

(CR) will subsequently experience recurrence (72). Only 20% of these may be diagnosed at routine surveillance imaging in asymptomatic patients, whereas the other 80% occur in symptomatic patients. However, the prognosis in these groups of patients may be similar (72). Therefore, there remains some uncertainty about the optimal follow-up strategy after treatment.

In about 50% of recurrences, new lesions are noted, distant to the original tumor site (73), and more than half of unilateral cases may recur with bilateral lesions (74). This reflects the fact that this disease affects the entire CNS, as shown in autopsies with microscopic tumor infiltration in non-enhancing T2-hyperintense and T2 normal areas (75), in contrast to most other CNS tumors. Effective treatments therefore require prescription to the entire CNS in the form of chemotherapy or less commonly whole brain radiation therapy—in contrast, GBMs and other HGGs require only targeted partial brain radiation.

Most first recurrences occur <5 years after initial treatment. After treatment, patients should be scanned every 3 months for the next 2 years, every 6 months for the following 3 years, and then once each year for the following 5 years. Overall, surveillance for primary CNS lymphoma recurrence is recommended for 10 years. Of note, late relapsing disease has been observed more than 5 years after initial diagnosis (76). During these follow-up appointments, patients should receive a standard physical exam and history, as well as a gadolinium-enhanced MRI, and those who have had any ophthalmologic or spinal involvement should receive additional evaluation (69).

Interesting imaging patterns may be observed on follow-up MRI: After successful treatment, nearly two-thirds of patients treated with MTX will demonstrate residual pre-contrast T1-hyperintense changes (77). These changes are unrelated to hemorrhage, and instead are possibly related to oxidative stress induced by free radicals and/or due to sulfur-containing excitatory amino acid-induced N-methyl-D-aspartate (NMDA) receptor stimulation, leading to increased intracellular calcium (78).

Prognosis

To guide patient prognosis and treatment discussions, the two most commonly used prognostic scores are the Memorial Sloan Kettering Cancer Center (MSK) prognostic score and the International Extranodal Lymphoma Study Group (IELSG) score (79,80). The clinical MSK prognostic score predicts worse prognosis based on age >50 years and Karnofsky performance score <70. The IELSG score predicts worse prognosis with deep brain involvement (periventricular regions, basal ganglia, brainstem, and/or cerebellum), which occurs in one-third of patients who have a worse odds ratio (OR) of 1.45 (95% CI: 1.11–1.9) (69). The IELSG score also predicts worse prognosis with age >60 years, poor performance status, high LDH in serum, and high protein in CSF. Both scoring systems predict worse prognosis in the elderly, who have an increasing incidence of primary CNS lymphoma (15,81). Although not incorporated into either scoring system, imaging abnormalities such as infratentorial location, large enhancing lesions, and smaller decreases in enhancement after treatment also suggest worse outcomes (29). Leptomeningeal spread does not portend a worse prognosis in primary CNS lymphoma patients (48), unlike the very poor prognosis resulting from leptomeningeal spread in patients with systemic non-Hodgkin lymphoma.

PET imaging

PET imaging offers additional value to cross-sectional imaging studies in neuro-oncology, as it enables the non-invasive evaluation of molecular and metabolic features of brain tumors. [^{18}F]-FDG PET is currently the only FDA-approved imaging modality for brain tumors. Historically, it has been used to differentiate radiation necrosis from tumor recurrence of enhancing brain lesions on MRI, distinguish glioma from CNS lymphoma, and diagnose opportunistic infections. Procedure guidelines and descriptions of findings in brain tumor imaging should generally comply with previously published guidelines for FDG imaging in oncology (82).

PET systems provide static, dynamic, or gated images of the distribution of positron-emitting radionuclides within the body by detecting pairs of photons produced by the coincident annihilation of a positron and an electron. Images are generated by a reconstruction process using the coincidence pair data. PET is generally combined with CT in a single system (PET/CT). Combined PET/MRI systems are currently less widely available. The patient's head should be positioned in a dedicated holder with the arms along the body, and the entire brain should be in the field of view. Commonly, for brain FDG PET, a static image is acquired for 10–20 min, at least 45 min after FDG injection, with a transaxial 128×128 or finer matrix size. After image acquisition and reconstruction, using appropriate

calibration factors, quantitative images are obtained as each pixel represents an activity concentration (Bq/mL). Dynamic FDG PET studies require a dynamic acquisition for about 60 min. Imaging data are analyzed using a tracer kinetic model (and in the case of FDG sometimes a correction factor, termed lumped constant, to account for differences in substrate utilization between glucose and FDG). Dynamic PET enables true quantification of blood flow, metabolism, proliferation, and other processes (83-86). Kinetic analysis of FDG PET parameters may be helpful for diagnosis of CNS lymphoma and for monitoring therapy response (87-89).

The majority of clinical brain PET studies are based on acquisition and visual evaluation of static images. PET parameters for lesion analysis include standardized uptake values (SUVs) (90) such as mean SUV (SUV_{mean}), maximum SUV (SUV_{max}) (volume encompassing the voxel with highest uptake), and peak SUV (SUV_{peak}) (approximately 1.2-cm diameter fixed size volume centered on the area with maximum uptake) as measures for the intensity of uptake, and volume-based parameters such as metabolic tumor volume (MTV) (volume encompassed by a defined isocontour around the voxel with the highest PET uptake) and total lesion glycolysis (TLG) (calculated by multiplying MTV by SUV_{mean}). Lesion-to-reference-region ratios using mean or maximum SUV can be used to provide a measure of FDG uptake in lesions. A few studies have suggested that delayed imaging of brain tumors (e.g., at 90–480 min) could augment the tumor-to-normal brain contrast (91,92), resulting in improved lesion detection at later imaging time points (93). However, delayed FDG PET imaging may not corroborate a presumptive diagnosis of primary CNS lymphoma, as false-positive uptake in two cases of demyelination has been observed (94).

Radiomics, or textural feature extraction, is an emerging technique for assessing intra-tumoral heterogeneity based on complex mathematical modeling of the spatial relationship between multiple image voxels (95,96). One recent retrospective study in 77 patients (primary CNS lymphoma: n=24; GBM: n=53) suggested that this analysis may help distinguish primary CNS lymphoma from GBM (97). Finally, studies reported an inverse relationship between PET parameters and MRI-derived ADC; however, the utility of DWI to improve diagnostic accuracy remains uncertain (98-100). In the following sections, we will only discuss data obtained with standard static imaging.

Imaging pattern on FDG PET

Primary CNS lymphoma lesions mostly show high FDG uptake, due to increased glucose metabolism as compared to normal brain tissue (*Figure 4*). This demand is met by enhanced cellular entry of nutrients through upregulation of specific transporters and enzymes. Tumor cells frequently overexpress glucose transporter GLUT1 and GLUT3 as well as hexokinase 2 (HK-2) (101,102). Preliminary data derived from biopsies performed in seven patients showed that SUV_{max} of FDG correlates with the mRNA expression level of glucose transporter GLUT3, but not GLUT1 (103). Subsequent studies performed in systemic lymphoma corroborated this finding (104,105). However, a recent study employing a panel of orthotopic, patient-derived xenograft models from both immunocompetent and EBV-positive primary CNS lymphoma biopsy specimens reported that GLUT1 and HK-2 were upregulated and highly correlated with FDG uptake (106).

Whereas cortical brain shows high FDG uptake (potentially interfering with the detection of FDG-avid brain lesions), most sites of CNS lymphoma are in fact located in the white matter, deep cerebral structures, and periventricular regions, suggesting that FDG PET may also be useful in the diagnosis and follow-up of this disease (107-109) (please see Table S1 for an overview of selected diagnostic studies). Primary CNS lymphoma lesions typically showed high uptake on PET with SUV_{max} ranging from 5–39. However, some lesions visualized on MRI had no correlate on FDG PET (31,107,110-112) due to, e.g., small lesion size (usually <1 cm) and their pattern on MRI, such as disseminated presentation. Furthermore, leptomeningeal disease and eye involvement, diagnosed on CSF flow cytometry and vitreous aspirate, are usually not detectable on PET (31), due to small volume of FDG-avid disease or prominent FDG uptake in adjacent physiologic structures. This is also true for lesions in proximity to basal ganglia, which exhibit high physiologic FDG uptake. In a study of 25 patients with recurrent disease (113), the sensitivity of detecting disease in the brain was 87% [13/15], spine/nerves 80% [4/5], and eyes only 20% [1/5]. Conversely, some FDG-avid lesions may only be seen on FLAIR MR images but not on contrast-enhanced T2-weighted images (111).

A recent systematic review and meta-analysis of eight retrospective studies involving a total of 129 patients (114)

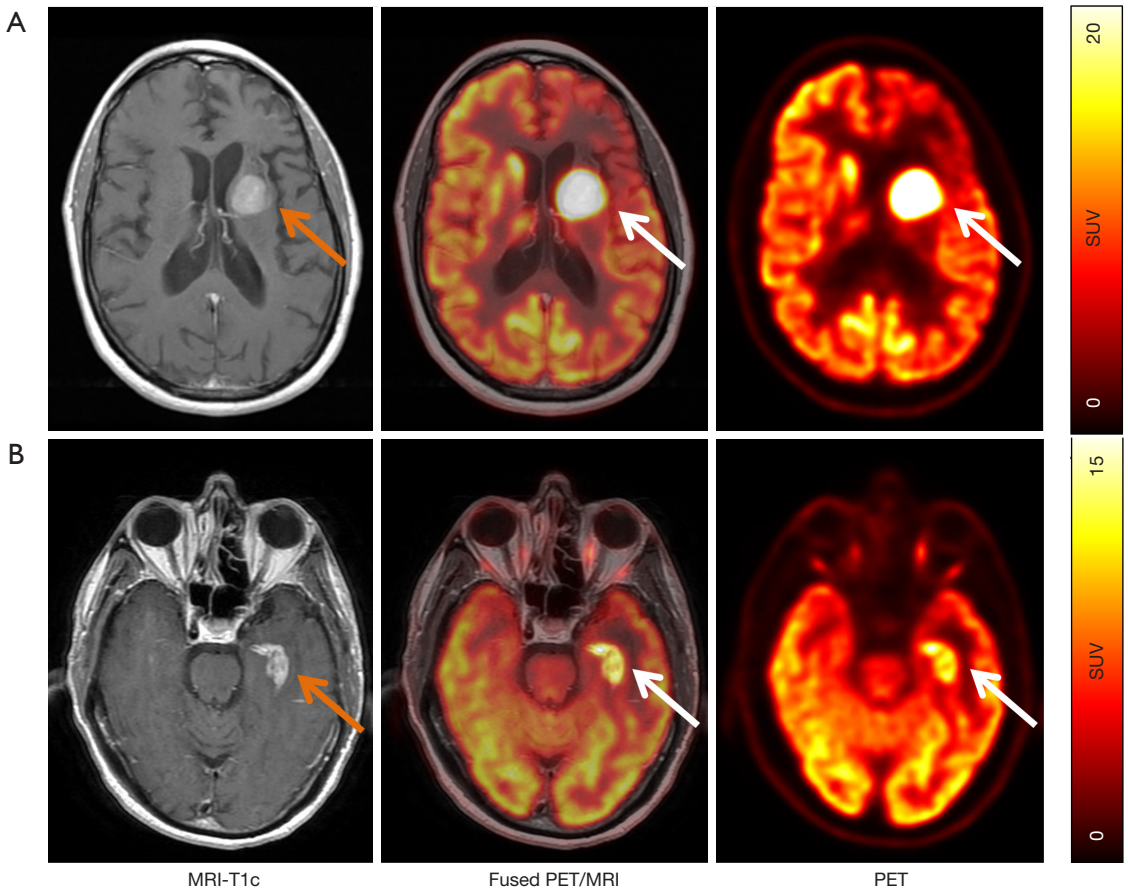

Figure 4 Representative cases of primary CNS lymphoma on FDG PET and MRI. (A) Contrast-enhanced T1-weighted MRI shows an enhancing lesion (left, orange arrow) in left corona radiata and superior basal ganglia, which demonstrate focal [^{18}F]-FDG uptake on axial fused PET/MRI (middle, white arrows) and PET images. (B) Contrast-enhanced T1-weighted MRI depicts an enhancing lesion (left, orange arrow) at the left temporal horn; fused PET/MRI (middle, white arrow) and PET images confirmed focal [^{18}F]-FDG uptake. MRI, magnetic resonance imaging; PET, positron emission tomography; CNS, central nervous system; FDG, fluorodeoxyglucose.

reported a pooled sensitivity of 0.88 (95% CI: 0.80–0.94), specificity of 0.86 (95% CI: 0.73–0.94), positive likelihood ratio (positive LR)* of 3.99 (95% CI: 2.31–6.90), negative likelihood ratio (negative LR)** of 0.11 (95% CI: 0.04–0.32), and diagnostic OR*** of 33.40 (95% CI: 10.40–107.3) (115,116). In addition, the AUC and Q index were 0.9192 and 0.8525, respectively.

The utility of whole-body FDG PET/CT for the staging and detection of lymphoma outside the brain has been corroborated in several studies. Indeed, FDG PET/CT has shown that about 4–10% of patients with suspected lymphoma confined to the brain have systemic involvement (31,117).

Differentiating common enhancing brain lesions

The role of FDG PET to characterize contrast-enhancing

* Positive LR = the probability of a person who has the disease testing positive divided by the probability of a person who does not have the disease testing positive;

** Negative LR = the probability of a person who has the disease testing negative divided by the probability of a person who does not have the disease testing negative;

*** OR = measure of the effectiveness of a diagnostic test.

brain lesions on CT and MRI has been investigated intensively. For instance, in immunocompromised patients with AIDS, FDG uptake in brain lymphoma can be used to discriminate between HIV-related brain disease, such as toxoplasmosis, and primary CNS lymphoma. Since 1990, multiple studies have shown that higher FDG uptake in CNS lymphoma enables differentiation from non-malignant etiologies in immunocompromised patients (118-120). In immunocompetent patients, FDG PET may help differentiate primary CNS lymphoma lesions from other brain neoplasms. For instance, in a study of 34 patients (including 7 lymphomas, 9 HGGs, and 18 metastatic tumors) (121), SUV_{max}, SUV_{mean}, and tumor-to-normal-tissue ratios were higher in lymphoma than in other tumors. Using an SUV_{max} of 15.0 as a cutoff for diagnosing primary CNS lymphoma, only one HGG was found to be false-positive.

In another study with 101 patients (including 25 patients with lymphoma), an SUV_{max} cut-off of 15.5 had 84% sensitivity and 80% specificity for diagnosing lymphomas (122). Finally, in a prospective study in 49 patients (31), 26 (53%) patients were found to have DLBCL-type CNS lymphoma, and the remaining 23 (47%) had other diagnoses such as HGG (n=17), infectious/inflammatory pathology (n=4), or brain metastases (n=2). CNS lymphoma was unifocal in 50% and multifocal in the other 50%. The mean SUV_{max} (27.5 *vs.* 18.2; P=0.001) and mean tumor/normal tissue (T/N) ratio [defined as SUV_{max}(lesion)/SUV_{max} (contralateral hemisphere within normal brain) (2.34 *vs.* 1.53; P<0.001)] of CNS lymphoma was significantly higher than that of other histologic diagnoses. An "optimal cut-off" for SUV_{max} (18.8) and T/N ratio (1.66) provided an overall accuracy of 75% (95% CI: 65–90%) and 83% (95% CI: 72–94%), respectively.

In summary, primary CNS lymphoma exhibits higher FDG uptake compared to other disease entities (GBM, metastases, and inflammatory/infectious lesions) that may not be reliably distinguished on conventional neuroimaging studies such as MRI. Nevertheless, any recommendations regarding specific SUV cut-offs for differentiating between various diseases must be considered with caution, as they require confirmation in prospective studies and are subject to a variety of technical factors related to PET acquisition and image reconstruction.

Response assessment

Few studies have investigated the utility of FDG PET/CT for monitoring response, mostly for MTX-based treatments, and detection of recurrence (88,110,111,113,123).

While SUVs and tumor burden measured on FDG PET/CT have been identified as prognostic factors in patients with systemic lymphoma (124-127), data on CNS lymphoma are still scarce. So far, mostly retrospective studies have explored the prognostic role of FDG PET in this setting (108,123,128-130). One retrospective study in 52 patients with untreated primary CNS lymphoma reported that PFS and OS were shorter in patients with larger MTV (cut-off 9.8 cm^3) and higher TLG (108). Another retrospective study in 42 patients with newly diagnosed primary CNS lymphoma reported an inverse correlation between high uptake on baseline FDG PET and survival (129).

A larger retrospective study evaluated the prognostic value of interim PET/CT (i-PET/CT) and end-of-treatment PET/CT in 66 patients with primary CNS lymphoma receiving MTX-based treatments (123). Only the end-of-treatment PET was associated with patient outcome.

Our group prospectively investigated the value of baseline FDG PET in 53 patients with recurrent/refractory (r/r) CNS lymphoma, including 34 patients with r/r primary CNS lymphoma prior to receiving ibrutinib-based therapies. At baseline, two-thirds of the patients had FDG-avid lesions. In the remaining patients, small lesion size limited visualization on PET. In the patients with measurable lesions, PET parameters SUV_{max}, TLG, and MTV correlated with PFS, in that higher lesional metabolic parameters were inversely related to patient outcome (131).

Radiolabeled amino acids for imaging CNS lymphoma

In addition to FDG, radiolabeled amino acids such as ^{11}C-methyl-L-methionine (MET), ^{18}F-fluoroethyl-L-tyrosine (FET), and ^{18}F-fluoro-L-dihydroxyphenylalanine (DOPA) are used for brain tumor imaging, offering the distinct advantage of minimal uptake in normal brain parenchyma. In some studies, amino acid PET was able to differentiate intracranial neoplasms (including glioma, lymphoma, and metastasis), which typically demonstrate high tracer uptake, from non-neoplastic etiologies (69,132-135). For imaging CNS lymphoma, MET has been used in a few studies (136-140). The L-type amino acid transporter 1 (LAT1), which mediates transport of amino acids including MET into cells, is strongly expressed in many cancer cells and a correlation between the expression of LAT1 and MET SUV_{max} in primary CNS lymphoma has been reported (103).

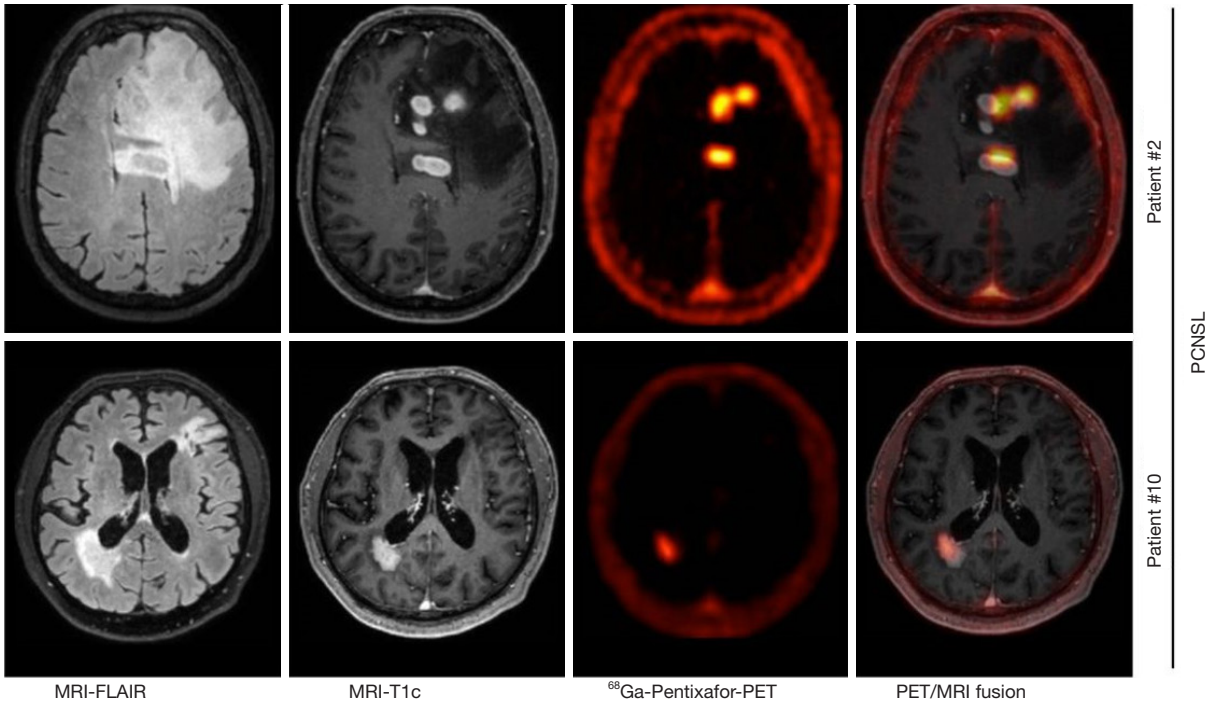

Figure 5 Representative cases of primary CNS lymphoma on CXCR4-directed PET and MRI. Depicted are representative MR images (T1c and FLAIR sequences) and the corresponding CXCR4-directed PET images and the fusion of MRI (FLAIR) and PET of two patients with primary CNS lymphoma. This research was originally published in *J Nucl Med* (Herhaus *et al.* (145)]. Modified with permission of *J Nucl Med*. MRI, magnetic resonance imaging; FLAIR, fluid-attenuated inversion recovery; MRI, magnetic resonance imaging; CNS, central nervous system; CXCR4, C-X-C chemokine receptor 4.

While both FDG and MET showed similar detection rates of primary CNS lymphoma lesions, the lesional tracer uptake was higher with FDG than with MET (88,136,137). Moreover, the higher FDG uptake in primary CNS lymphoma enabled differentiation of this disease from GBM, whereas more sophisticated kinetic analysis might be needed to achieve the same for MET (133,140).

Few studies have investigated the role of MET PET for response assessment (139,141,142). One prospective study in 26 patients (139) assessed the value of interim MET PET/CT and MRI after four cycles of high dose-MTX-based induction chemotherapy and noted an interim response discrepancy between MET PET and brain MRI in four patients, with a negative PET but MR showing contrast-enhancing lesions. All four patients achieved complete remission following treatment; thus, PET may enable detection of response at an earlier timepoint. One study also suggested that MET PET/CT may enable prediction of patient outcome (139).

Emerging PET tracers

New radiotracers with potentially higher sensitivity and/or specificity are being explored, including [^{11}C]-choline (143), prostate-specific membrane antigen (PSMA) (144), C-X-C chemokine receptor 4 (CXCR4) (145), and fludarabine (FDB) (146). CXCR-4 is a transmembrane chemokine receptor and with its ligand CXCL12 functions as master regulator of leukocyte migration, homing and hematopoietic stem and progenitor cell retention in bone marrow niches. Dysregulation of the CXCR4-CXCL12 axis in tumor cells can promote cell migration and proliferation and induction of metastasis. Treatments with CXCR4 antagonists for various malignancies are under active investigation. Primary CNS lymphoma cells have been shown to consistently express CXCR4 (147). In a recent proof-of-concept study, 11 patients with CNS lymphoma (primary CNS lymphoma, n=8; secondary CNS lymphoma, n=3) were imaged with the CXCR4-directed PET tracer ^{68}Ga-pentixafor and excellent lesion-to-normal brain contrast was observed (*Figure 5*) (145).

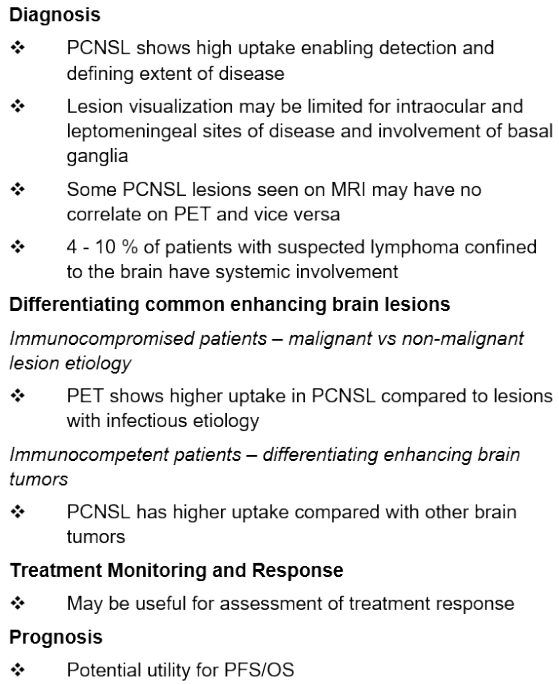

Figure 6 Role of FDG PET—Key points. PCNSL, primary central nervous system lymphoma; PET, positron emission tomography; PFS, progression-free survival; OS, overall survival; FDG, fluorodeoxyglucose.

Furthermore, CXCR4 uptake on baseline PET correlated with treatment response, suggesting that ^{68}Ga-pentixafor PET may serve as a tool for response and risk assessment in patients with CNS lymphoma.

[^{18}F]-FDB, an adenine nucleoside analog, has been developed as a novel PET imaging probe to overcome limitations in imaging. 9-β-D-Arabinofuranosyl-2-fluoroadenine monophosphate (FDB monophosphate) was first developed as a class of anticancer nucleoside analogues in the 1960s (148,149). It is used to treat indolent B-cell malignancies (150) and as a conditioning regimen prior to stem cell transplants due to its potent immunosuppressive activity promoting lymphocyte depletion (151). As this drug possesses a ^{19}F atom on the base moiety, substitution by a ^{18}F atom generates a positron-emitting radiotracer without any modification to its pharmacokinetic and pharmacodynamic profiles (152). This probe is a substrate for the equilibrative nucleoside transporters, ENT1 and ENT2. After transport into the cell and initial phosphorylation by deoxycytidine kinase (dCK), an enzyme expressed at relatively high levels in lymphoid malignancies, the FDB is trapped. In a preclinical study (146) using intracranially implanted human xenografts of primary CNS lymphoma and GBM, FDB PET demonstrated higher specificity for primary CNS lymphoma, whereas FDG uptake was similar in primary CNS lymphoma and GBM xenografts—in contrast to clinical data in humans.

Conclusions and future directions

Primary CNS lymphoma can have highly variable appearances on MRI. Early imaging diagnosis of possible primary CNS lymphoma is necessary for proper management, which includes avoidance of corticosteroids and consideration of biopsy rather than attempted gross total resection. Advanced MRI techniques (such as MR diffusion, perfusion spectroscopy) provide further insights into tumor biology and physiology and may be useful in distinguishing primary CNS lymphoma from other etiologies. Newly emerging techniques, such as radiomics, machine learning, and other forms of artificial intelligence may potentially aid in differential diagnosis and prognostication in the future (153,154). Nevertheless, contrast-enhanced MRI is the standard modality in neuro-oncologic imaging used for patient management.

On PET, most primary CNS lymphoma lesions show prominent FDG uptake; therefore, FDG PET can be used for diagnosing this disease and defining its extent (*Figure 6*). Some (particularly smaller) lesions seen on MRI may not be apparent on FDG PET. On the other hand, some lesions noted on PET may not be identified (or are perhaps initially overlooked or misinterpreted) on standard MRI. Therefore, PET and MRI provide complementary information in CNS lymphoma. Ideally, patients with primary CNS lymphoma should be imaged on a combined PET/MR scanner to obtain complete information in one imaging session.

Acknowledgments

Funding: SK was supported in part by the NIH/NCI Paul Calabresi Career Development Award for Clinical Oncology (K12 CA184746) and the National Institutes of Health Lymphoma SPORE (P50 CA192937). CG was supported by grants from Cycle for Survival Equinox and the Leukemia & Lymphoma Society. This study was also supported in part by the NIH/NCI Cancer Center Support Grant (P30 CA008748).

Footnote

Provenance and Peer Review: This article was commissioned

by the Guest Editors (Andrés J. M. Ferreri, Maurilio Ponzoni) for the series "Central Nervous System Lymphomas" published in *Annals of Lymphoma*. The article has undergone external peer review.

Reporting Checklist: The authors have completed the Narrative Review reporting checklist. Available at http://dx.doi.org/10.21037/aol-20-52

Conflicts of Interest: All authors have completed the ICMJE uniform disclosure form (available at http://dx.doi.org/10.21037/aol-20-52). The series "Central Nervous System Lymphomas" was commissioned by the editorial office without any funding or sponsorship. RJY reports grants and personal fees from Agios, personal fees from Puma, personal fees from NordicNeuroLab, personal fees from ICON plc, outside the submitted work. CG reports personal fees from BTG, personal fees from Kite, personal fees from American Academy of Neurology, personal fees from Ono, outside the submitted work. The authors have no other conflicts of interest to declare.

Ethical Statement: The authors are accountable for all aspects of the work in ensuring that questions related to the accuracy or integrity of any part of the work are appropriately investigated and resolved.

References

1. Ostrom QT, Gittleman H, Xu J, et al. CBTRUS statistical report: Primary brain and other central nervous system tumors diagnosed in the United States in 2009-2013. Neuro Oncol 2016;18:v1-75.
2. Miller DC, Hochberg FH, Harris NL, et al. Pathology with clinical correlations of primary central nervous system non-Hodgkin's lymphoma. The Massachusetts General Hospital experience 1958-1989. Cancer 1994;74:1383-97.
3. Camilleri-Broët S, Martin A, Moreau A, et al. Primary central nervous system lymphomas in 72 immunocompetent patients: pathologic findings and clinical correlations. Groupe Ouest Est d'étude des Leucénies et Autres Maladies du Sang (GOELAMS). Am J Clin Pathol 1998;110:607-12.
4. Villano JL, Koshy M, Shaikh H, et al. Age, gender, and racial differences in incidence and survival in primary CNS lymphoma. Br J Cancer 2011;105:1414-8.
5. Schabet M. Epidemiology of primary CNS lymphoma. J Neurooncol 1999;43:199-201.
6. Mansour A, Qandeel M, Abdel-Razeq H, et al. MR imaging features of intracranial primary CNS lymphoma in immune competent patients. Cancer Imaging 2014;14:22.
7. Bayraktar S, Bayraktar UD, Ramos JC, et al. Primary CNS lymphoma in HIV positive and negative patients: comparison of clinical characteristics, outcome and prognostic factors. J Neurooncol 2011;101:257-65.
8. Olson JE, Janney CA, Rao RD, et al. The continuing increase in the incidence of primary central nervous system non-Hodgkin lymphoma: a surveillance, epidemiology, and end results analysis. Cancer 2002;95:1504-10.
9. Kadan-Lottick NS, Skluzacek MC, Gurney JG. Decreasing incidence rates of primary central nervous system lymphoma. Cancer 2002;95:193-202.
10. Alizadeh AA, Eisen MB, Davis RE, et al. Distinct types of diffuse large B-cell lymphoma identified by gene expression profiling. Nature 2000;403:503-11.
11. Abrey LE, DeAngelis LM, Yahalom J. Long-term survival in primary CNS lymphoma. J Clin Oncol 1998;16:859-63.
12. O'Brien P, Roos D, Pratt G, et al. Phase II multicenter study of brief single-agent methotrexate followed by irradiation in primary CNS lymphoma. J Clin Oncol 2000;18:519-26.
13. Brada M, Hjiyiannakis D, Hines F, et al. Short intensive primary chemotherapy and radiotherapy in sporadic primary CNS lymphoma (PCL). Int J Radiat Oncol Biol Phys 1998;40:1157-62.
14. Roth P, Martus P, Kiewe P, et al. Outcome of elderly patients with primary CNS lymphoma in the G-PCNSL-SG-1 trial. Neurology 2012;79:890-6.
15. Mendez JS, Ostrom QT, Gittleman H, et al. The elderly left behind-changes in survival trends of primary central nervous system lymphoma over the past 4 decades. Neuro Oncol 2018;20:687-94.
16. Grommes C, Tang SS, Wolfe J, et al. Phase 1b trial of an ibrutinib-based combination therapy in recurrent/refractory CNS lymphoma. Blood 2019;133:436-45.

17. Rubenstein JL, Geng H, Fraser EJ, et al. Phase 1 investigation of lenalidomide/rituximab plus outcomes of lenalidomide maintenance in relapsed CNS lymphoma. Blood Adv 2018;2:1595-607.
18. Ghesquieres H, Chevrier M, Laadhari M, et al. Lenalidomide in combination with intravenous rituximab (REVRI) in relapsed/refractory primary CNS lymphoma or primary intraocular lymphoma: a multicenter prospective 'proof of concept' phase II study of the French Oculo-Cerebral lymphoma (LOC) Network and the Lymphoma Study Association (LYSA)†. Ann Oncol 2019;30:621-8.
19. Grommes C, DeAngelis LM. Primary CNS lymphoma. J Clin Oncol 2017;35:2410-8.
20. Fischer L, Martus P, Weller M, et al. Meningeal dissemination in primary CNS lymphoma: prospective evaluation of 282 patients. Neurology 2008;71:1102-8.
21. Bessell EM, Hoang-Xuan K, Ferreri AJ, et al. Primary central nervous system lymphoma: biological aspects and controversies in management. Eur J Cancer 2007;43:1141-52.
22. Baraniskin A, Kuhnhenn J, Schlegel U, et al. Identification of microRNAs in the cerebrospinal fluid as marker for primary diffuse large B-cell lymphoma of the central nervous system. Blood 2011;117:3140-6.
23. Baraniskin A, Kuhnhenn J, Schlegel U, et al. Identification of microRNAs in the cerebrospinal fluid as biomarker for the diagnosis of glioma. Neuro Oncol 2012;14:29-33.
24. Eichler AF, Batchelor TT. Primary central nervous system lymphoma: presentation, diagnosis and staging. Neurosurg Focus 2006;21:E15.
25. Korfel A, Elter T, Thiel E, et al. Phase II study of central nervous system (CNS)-directed chemotherapy including high-dose chemotherapy with autologous stem cell transplantation for CNS relapse of aggressive lymphomas. Haematologica 2013;98:364-70.
26. Chen YB, Batchelor T, Li S, et al. Phase 2 trial of high-dose rituximab with high-dose cytarabine mobilization therapy and high-dose thiotepa, busulfan, and cyclophosphamide autologous stem cell transplantation in patients with central nervous system involvement by non-Hodgkin lymphoma. Cancer 2015;121:226-33.
27. Ferreri AJ, Donadoni G, Cabras MG, et al. High doses of antimetabolites followed by high-dose sequential chemoimmunotherapy and autologous stem-cell transplantation in patients with systemic B-cell lymphoma and secondary CNS involvement: final results of a multicenter phase II trial. J Clin Oncol 2015;33:3903-10.
28. Grommes C, Rubenstein JL, DeAngelis LM, et al. Comprehensive approach to diagnosis and treatment of newly diagnosed primary CNS lymphoma. Neuro Oncol 2019;21:296-305.
29. Chiavazza C, Pellerino A, Ferrio F, et al. Primary CNS lymphomas: Challenges in diagnosis and monitoring. Biomed Res Int 2018;2018:3606970.
30. Suh CH, Kim HS, Park JE, et al. Primary central nervous system lymphoma: diagnostic yield of whole-body CT and FDG PET/CT for initial systemic imaging. Radiology 2019;292:440-6.
31. Gupta M, Gupta T, Purandare N, et al. Utility of flouro-deoxy-glucose positron emission tomography/computed tomography in the diagnostic and staging evaluation of patients with primary CNS lymphoma. CNS Oncol 2019;8:CNS46.
32. Kim DS, Na DG, Kim KH, et al. Distinguishing tumefactive demyelinating lesions from glioma or central nervous system lymphoma: added value of unenhanced CT compared with conventional contrast-enhanced MR imaging. Radiology 2009;251:467-75.
33. Hoang-Xuan K, Bessell E, Bromberg J, et al. Diagnosis and treatment of primary CNS lymphoma in immunocompetent patients: guidelines from the European Association for Neuro-Oncology. Lancet Oncol 2015;16:e322-32.
34. Fukuoka H, Hirai T, Okuda T, et al. Comparison of the added value of contrast-enhanced 3D fluid-attenuated inversion recovery and magnetization-prepared rapid acquisition of gradient echo sequences in relation to conventional postcontrast T1-weighted images for the evaluation of leptomeningeal diseases at 3T. AJNR Am J Neuroradiol 2010;31:868-73.
35. Utz MJ, Tamber MS, Mason GE, et al. Contrast-enhanced 3-dimensional fluid-attenuated inversion recovery sequences have greater sensitivity for detection of leptomeningeal metastases in pediatric brain tumors compared with conventional spoiled gradient echo sequences. J Pediatr Hematol Oncol 2018;40:316-9.
36. Ellingson BM, Bendszus M, Boxerman J, et al. Consensus recommendations for a standardized brain tumor imaging protocol in clinical trials. Neuro Oncol 2015;17:1188-98.
37. Barajas RF Jr, Rubenstein JL, Chang JS, et al. Diffusion-weighted MR imaging derived apparent diffusion coefficient is predictive of clinical outcome in primary central nervous system lymphoma. AJNR Am J Neuroradiol 2010;31:60-6.
38. Toh CH, Castillo M, Wong AM, et al. Primary cerebral lymphoma and GBM multiforme: differences in diffusion

characteristics evaluated with diffusion tensor imaging. AJNR Am J Neuroradiol 2008;29:471-5.
39. Lee IH, Kim ST, Kim HJ, et al. Analysis of perfusion weighted image of CNS lymphoma. Eur J Radiol 2010;76:48-51.
40. Boxerman JL, Quarles CC, Hu LS, et al. Consensus recommendations for a dynamic susceptibility contrast MRI protocol for use in high-grade gliomas. Neuro Oncol 2020;22:1262-75.
41. Liu D, Liu X, Ba Z, et al. Delayed contrast enhancement in magnetic resonance imaging and vascular morphology of primary diffuse large B-cell lymphoma (DLBCL) of the central nervous system (CNS): A retrospective study. Med Sci Monit 2019;25:3321-8.
42. Hatzoglou V, Oh JH, Buck O, et al. Pretreatment dynamic contrast-enhanced MRI biomarkers correlate with progression-free survival in primary central nervous system lymphoma. J Neurooncol 2018;140:351-8.
43. Valles FE, Perez-Valles CL, Regalado S, et al. Combined diffusion and perfusion MR imaging as biomarkers of prognosis in immunocompetent patients with primary central nervous system lymphoma. AJNR Am J Neuroradiol 2013;34:35-40.
44. Haldorsen IS, Espeland A, Larsson EM. Central nervous system lymphoma: Characteristic findings on traditional and advanced imaging. AJNR Am J Neuroradiol 2011;32:984-92.
45. Bataille B, Delwail V, Menet E, et al. Primary intracerebral malignant lymphoma: Report of 248 cases. J Neurosurg 2000;92:261-6.
46. Taylor JW, Flanagan EP, O'Neill BP, et al. Primary leptomeningeal lymphoma: International Primary CNS Lymphoma Collaborative Group report. Neurology 2013;81:1690-6.
47. Kerbauy MN, Moraes FY, Lok BH, et al. Challenges and opportunities in primary CNS lymphoma: A systematic review. Radiother Oncol 2017;122:352-61.
48. Korfel A, Weller M, Martus P, et al. Prognostic impact of meningeal dissemination in primary CNS lymphoma (PCNSL): experience from the G-PCNSL-SG1 trial. Ann Oncol 2012;23:2374-80.
49. Lin X, Lee M, Buck O, et al. Diagnostic accuracy of T1-weighted dynamic contrast-enhanced-MRI and DWI-ADC for differentiation of glioblastoma and primary CNS lymphoma. AJNR Am J Neuroradiol 2017;38:485-91.
50. Lu X, Xu W, Wei Y, et al. Diagnostic performance of DWI for differentiating primary central nervous system lymphoma from glioblastoma: A systematic review and meta-analysis. Neurol Sci 2019;40:947-56.
51. Xu W, Wang Q, Shao A, et al. The performance of MR perfusion-weighted imaging for the differentiation of high-grade glioma from primary central nervous system lymphoma: A systematic review and meta-analysis. PLoS One 2017;12:e0173430.
52. Wu Y, Den Z, Lin Y. Accuracy of susceptibility-weighted imaging and dynamic susceptibility contrast magnetic resonance imaging for differentiating high-grade glioma from primary central nervous system lymphomas: Meta-analysis. World Neurosurg 2018;112:e617-23.
53. Murayama K, Nishiyama Y, Hirose Y, et al. Differentiating between central nervous system lymphoma and high-grade glioma using dynamic susceptibility contrast and dynamic contrast-enhanced MR imaging with histogram analysis. Magn Reson Med Sci 2018;17:42-9.
54. You SH, Yun TJ, Choi HJ, et al. Differentiation between primary CNS lymphoma and glioblastoma: qualitative and quantitative analysis using arterial spin labeling MR imaging. Eur Radiol 2018;28:3801-10.
55. Harting I, Hartmann M, Jost G, et al. Differentiating primary central nervous system lymphoma from glioma in humans using localised proton magnetic resonance spectroscopy. Neurosci Lett 2003;342:163-6.
56. Sawlani V, Patel MD, Davies N, et al. Multiparametric MRI: Practical approach and pictorial review of a useful tool in the evaluation of brain tumours and tumour-like lesions. Insights Imaging 2020;11:84.
57. da Rocha AJ, Sobreira Guedes BV, da Silveira da Rocha TM, et al. Modern techniques of magnetic resonance in the evaluation of primary central nervous system lymphoma: contributions to the diagnosis and differential diagnosis. Rev Bras Hematol Hemoter 2016;38:44-54.
58. Ko CC, Tai MH, Li CF, et al. Differentiation between glioblastoma multiforme and primary cerebral lymphoma: Additional benefits of quantitative diffusion-weighted MR imaging. PLoS One 2016;11:e0162565.
59. Chawla S, Zhang Y, Wang S, et al. Proton magnetic resonance spectroscopy in differentiating glioblastomas from primary cerebral lymphomas and brain metastases. J Comput Assist Tomogr 2010;34:836-41.
60. Arevalo-Perez J, Peck KK, Young RJ, et al. Dynamic contrast-enhanced perfusion MRI and diffusion-weighted imaging in grading of gliomas. J Neuroimaging 2015;25:792-8.
61. Jung BC, Arevalo-Perez J, Lyo JK, et al. Comparison of glioblastomas and brain metastases using dynamic contrast-enhanced perfusion MRI. J Neuroimaging 2016;26:240-6.

62. Lu SS, Kim SJ, Kim HS, et al. Utility of proton MR spectroscopy for differentiating typical and atypical primary central nervous system lymphomas from tumefactive demyelinating lesions. AJNR Am J Neuroradiol 2014;35:270-7.
63. Naeem SB, Niazi F, Baig A, et al. Primary CNS lymphoma vs. tumefactive multiple sclerosis: A diagnostic challenge. J Coll Physicians Surg Pak 2018;28:66-8.
64. Saini J, Chatterjee S, Thomas B, et al. Conventional and advanced magnetic resonance imaging in tumefactive demyelination. Acta Radiol 2011;52:1159-68.
65. Ding Y, Xing Z, Liu B, et al. Differentiation of primary central nervous system lymphoma from high-grade glioma and brain metastases using susceptibility-weighted imaging. Brain Behav 2014;4:841-9.
66. Neska-Matuszewska M, Bladowska J, S siadek M, et al. Differentiation of glioblastoma multiforme, metastases and primary central nervous system lymphomas using multiparametric perfusion and diffusion MR imaging of a tumor core and a peritumoral zone-Searching for a practical approach. PLoS One 2018;13:e0191341.
67. Shim WH, Kim HS, Choi CG, et al. Comparison of apparent diffusion coefficient and intravoxel incoherent motion for differentiating among glioblastoma, metastasis, and lymphoma focusing on diffusion-related parameter. PLoS One 2015;10:e0134761.
68. Chen H, Dong H. A rare case of nonenhancing primary central nervous system lymphoma mimic multiple sclerosis. Neurosciences (Riyadh) 2015;20:380-4.
69. Abrey LE, Batchelor TT, Ferreri AJ, et al. Report of an international workshop to standardize baseline evaluation and response criteria for primary CNS lymphoma. J Clin Oncol 2005;23:5034-43.
70. Eisenhauer EA, Therasse P, Bogaerts J, et al. New response evaluation criteria in solid tumours: revised RECIST guideline (version 1.1). Eur J Cancer 2009;45:228-47.
71. Wen PY, Macdonald DR, Reardon DA, et al. Updated response assessment criteria for high-grade gliomas: response assessment in neuro-oncology working group. J Clin Oncol 2010;28:1963-72.
72. Fossard G, Ferlay C, Nicolas-Virelizier E, et al. Utility of post-therapy brain surveillance imaging in the detection of primary central nervous system lymphoma relapse. Eur J Cancer 2017;72:12-9.
73. Tabouret E, Houillier C, Martin-Duverneuil N, et al. Patterns of response and relapse in primary CNS lymphomas after first-line chemotherapy: Imaging analysis of the ANOCEF-GOELAMS prospective randomized trial. Neuro Oncol 2017;19:422-9.
74. Schulte-Altedorneburg G, Heuser L, Pels H. MRI patterns in recurrence of primary CNS lymphoma in immunocompetent patients. Eur J Radiol 2012;81:2380-5.
75. Chen JC, Gnepp DR, Bedrossian CW. Adenoid cystic carcinoma of the salivary glands: An immunohistochemical analysis. Oral Surg Oral Med Oral Pathol 1988;65:316-26.
76. Nayak L, Hedvat C, Rosenblum MK, et al. Late relapse in primary central nervous system lymphoma: Clonal persistence. Neuro Oncol 2011;13:525-9.
77. Karimi S, Hatzoglou V, Punia V, et al. Post-treatment T1 shortening in primary CNS lymphoma. J Neurooncol 2013;111:25-31.
78. Curras MC, Dingledine R. Selectivity of amino acid transmitters acting at N-methyl-D-aspartate and amino-3-hydroxy-5-methyl-4-isoxazolepropionate receptors. Mol Pharmacol 1992;41:520-6.
79. Abrey LE, Ben-Porat L, Panageas KS, et al. Primary central nervous system lymphoma: the Memorial Sloan-Kettering Cancer Center prognostic model. J Clin Oncol 2006;24:5711-5.
80. Ferreri AJ, Blay JY, Reni M, et al. Prognostic scoring system for primary CNS lymphomas: the International Extranodal Lymphoma Study Group experience. J Clin Oncol 2003;21:266-72.
81. Siegal T, Bairey O. Primary CNS lymphoma in the elderly: The challenge. Acta Haematol 2019;141:138-45.
82. Law I, Albert NL, Arbizu J, et al. Joint EANM/EANO/RANO practice guidelines/SNMMI procedure standards for imaging of gliomas using PET with radiolabelled amino acids and [(18)F]FDG: version 1.0. Eur J Nucl Med Mol Imaging 2019;46:540-57.
83. Dimitrakopoulou-Strauss A, Pan L, Sachpekidis C. Kinetic modeling and parametric imaging with dynamic PET for oncological applications: general considerations, current clinical applications, and future perspectives. Eur J Nucl Med Mol Imaging 2021;48:21-39.
84. Ullrich R, Backes H, Li H, et al. Glioma proliferation as assessed by 3'-fluoro-3'-deoxy-L-thymidine positron emission tomography in patients with newly diagnosed high-grade glioma. Clin Cancer Res 2008;14:2049-55.
85. Grkovski M, Kohutek ZA, Schöder H, et al. (18) F-Fluorocholine PET uptake correlates with pathologic evidence of recurrent tumor after stereotactic radiosurgery for brain metastases. Eur J Nucl Med Mol Imaging 2020;47:1446-57.
86. Grkovski M, Goel R, Krebs S, et al. Pharmacokinetic assessment of (18)F-(2S,4R)-4-fluoroglutamine in patients

with cancer. J Nucl Med 2020;61:357-66.
87. Nishiyama Y, Yamamoto Y, Monden T, et al. Diagnostic value of kinetic analysis using dynamic FDG PET in immunocompetent patients with primary CNS lymphoma. Eur J Nucl Med Mol Imaging 2007;34:78-86.
88. Kawai N, Nishiyama Y, Miyake K, et al. Evaluation of tumor FDG transport and metabolism in primary central nervous system lymphoma using [18F]fluorodeoxyglucose (FDG) positron emission tomography (PET) kinetic analysis. Ann Nucl Med 2005;19:685-90.
89. Kimura N, Yamamoto Y, Kameyama R, et al. Diagnostic value of kinetic analysis using dynamic 18F-FDG-PET in patients with malignant primary brain tumor. Nucl Med Commun 2009;30:602-9.
90. Boellaard R, O'Doherty MJ, Weber WA, et al. FDG PET and PET/CT: EANM procedure guidelines for tumour PET imaging: Version 1.0. Eur J Nucl Med Mol Imaging 2010;37:181-200.
91. Spence AM, Muzi M, Mankoff DA, et al. 18F-FDG PET of gliomas at delayed intervals: Improved distinction between tumor and normal gray matter. J Nucl Med 2004;45:1653-9.
92. Prieto E, Martí-Climent JM, Domínguez-Prado I, et al. Voxel-based analysis of dual-time-point 18F-FDG PET images for brain tumor identification and delineation. J Nucl Med 2011;52:865-72.
93. Jeanguillaume C, Metrard G, Rakotonirina H, et al. Delayed [(18)F]FDG PET imaging of central nervous system lymphoma: Is PET better than MRI? Eur J Nucl Med Mol Imaging 2006;33:1370-1.
94. Biswas S, Nagaraj C, Mangalore S, et al. Tumefactive demyelination versus primary central nervous system lymphoma on (18)F-fluorodeoxyglucose positron emission tomography magnetic resonance imaging: A twist in the tale. Indian J Nucl Med 2019;34:237-40.
95. Zaidi H, Alavi A, Naqa IE. Novel quantitative PET techniques for clinical decision support in oncology. Semin Nucl Med 2018;48:548-64.
96. Mayerhoefer ME, Umutlu L, Schöder H. Functional imaging using radiomic features in assessment of lymphoma. Methods 2021;188:105-11.
97. Kong Z, Jiang C, Zhu R, et al. (18)F-FDG-PET-based radiomics features to distinguish primary central nervous system lymphoma from glioblastoma. Neuroimage Clin 2019;23:101912.
98. Makino K, Hirai T, Nakamura H, et al. Does adding FDG-PET to MRI improve the differentiation between primary cerebral lymphoma and glioblastoma? Observer performance study. Ann Nucl Med 2011;25:432-8.
99. Matsushima N, Maeda M, Umino M, et al. Relation between FDG uptake and apparent diffusion coefficients in glioma and malignant lymphoma. Ann Nucl Med 2012;26:262-71.
100. Zhou W, Wen J, Hua F, et al. (18)F-FDG PET/CT in immunocompetent patients with primary central nervous system lymphoma: Differentiation from glioblastoma and correlation with DWI. Eur J Radiol 2018;104:26-32.
101. Yamamoto T, Seino Y, Fukumoto H, et al. Over-expression of facilitative glucose transporter genes in human cancer. Biochem Biophys Res Commun 1990;170:223-30.
102. Mathupala SP, Ko YH, Pedersen PL. Hexokinase II: Cancer's double-edged sword acting as both facilitator and gatekeeper of malignancy when bound to mitochondria. Oncogene 2006;25:4777-86.
103. Takahashi Y, Akahane T, Yamamoto D, et al. Correlation between positron emission tomography findings and glucose transporter 1, 3 and L-type amino acid transporter 1 mRNA expression in primary central nervous system lymphomas. Mol Clin Oncol 2014;2:525-9.
104. Khandani AH, Dunphy CH, Meteesatien P, et al. Glut1 and Glut3 expression in lymphoma and their association with tumor intensity on 18F-fluorodeoxyglucose positron emission tomography. Nucl Med Commun 2009;30:594-601.
105. Watanabe Y, Suefuji H, Hirose Y, et al. 18F-FDG uptake in primary gastric malignant lymphoma correlates with glucose transporter 1 expression and histologic malignant potential. Int J Hematol 2013;97:43-9.
106. Tateishi K, Miyake Y, Kawazu M, et al. A Hyperactive RelA/p65-Hexokinase 2 Signaling Axis Drives Primary Central Nervous System Lymphoma. Cancer Res 2020;80:5330-43.
107. Albano D, Bosio G, Bertoli M, et al. 18F-FDG PET/CT in primary brain lymphoma. J Neurooncol 2018;136:577-83.
108. Albano D, Bertoli M, Battistotti M, et al. Prognostic role of pretreatment 18F-FDG PET/CT in primary brain lymphoma. Ann Nucl Med 2018;32:532-41.
109. Kuwabara Y, Ichiya Y, Otsuka M, et al. High [18F]FDG uptake in primary cerebral lymphoma: a PET study. J Comput Assist Tomogr 1988;12:47-8.
110. de-Bonilla-Damiá Á, Fernández-López R, Capote-Huelva FJ, et al. Role of (18)F-FDG PET/CT in primary brain lymphoma. Rev Esp Med Nucl Imagen Mol 2017;36:298-303.
111. Palmedo H, Urbach H, Bender H, et al. FDG-PET in immunocompetent patients with primary central nervous system lymphoma: correlation with MRI and clinical follow-up. Eur J Nucl Med Mol Imaging 2006;33:164-8.

112. Maza S, Buchert R, Brenner W, et al. Brain and whole-body FDG-PET in diagnosis, treatment monitoring and long-term follow-up of primary CNS lymphoma. Radiol Oncol 2013;47:103-10.
113. Karantanis D, O'Eill B P, Subramaniam RM, et al. 18F-FDG PET/CT in primary central nervous system lymphoma in HIV-negative patients. Nucl Med Commun 2007;28:834-41.
114. Zou Y, Tong J, Leng H, et al. Diagnostic value of using 18F-FDG PET and PET/CT in immunocompetent patients with primary central nervous system lymphoma: A systematic review and meta-analysis. Oncotarget 2017;8:41518-28.
115. Glas AS, Lijmer JG, Prins MH, et al. The diagnostic odds ratio: A single indicator of test performance. J Clin Epidemiol 2003;56:1129-35.
116. McGee S. Simplifying likelihood ratios. J Gen Intern Med 2002;17:646-9.
117. Malani R, Bhatia A, Wolfe J, et al. Staging identifies non-CNS malignancies in a large cohort with newly diagnosed lymphomatous brain lesions. Leuk Lymphoma 2019;60:2278-82.
118. Hoffman JM, Waskin HA, Schifter T, et al. FDG-PET in differentiating lymphoma from nonmalignant central nervous system lesions in patients with AIDS. J Nucl Med 1993;34:567-75.
119. Heald AE, Hoffman JM, Bartlett JA, et al. Differentiation of central nervous system lesions in AIDS patients using positron emission tomography (PET). Int J STD AIDS 1996;7:337-46.
120. Villringer K, Jäger H, Dichgans M, et al. Differential diagnosis of CNS lesions in AIDS patients by FDG-PET. J Comput Assist Tomogr 1995;19:532-6.
121. Kosaka N, Tsuchida T, Uematsu H, et al. 18F-FDG PET of common enhancing malignant brain tumors. AJR Am J Roentgenol 2008;190:W365-9.
122. Purandare NC, Puranik A, Shah S, et al. Common malignant brain tumors: Can 18F-FDG PET/CT aid in differentiation? Nucl Med Commun 2017;38:1109-16.
123. Jo JC, Yoon DH, Kim S, et al. Interim (18)F-FGD PET/CT may not predict the outcome in primary central nervous system lymphoma patients treated with sequential treatment with methotrexate and cytarabine. Ann Hematol 2017;96:1509-15.
124. Vercellino L, Cottereau AS, Casasnovas O, et al. High total metabolic tumor volume at baseline predicts survival independent of response to therapy. Blood 2020;135:1396-405.
125. Ceriani L, Gritti G, Cascione L, et al. SAKK38/07 study: Integration of baseline metabolic heterogeneity and metabolic tumor volume in DLBCL prognostic model. Blood Adv 2020;4:1082-92.
126. Bailly C, Carlier T, Berriolo-Riedinger A, et al. Prognostic value of FDG-PET in patients with mantle cell lymphoma: Results from the LyMa-PET Project. Haematologica 2020;105:e33-6.
127. Moskowitz AJ, Schöder H, Gavane S, et al. Prognostic significance of baseline metabolic tumor volume in relapsed and refractory Hodgkin lymphoma. Blood 2017;130:2196-203.
128. Kawai N, Zhen HN, Miyake K, et al. Prognostic value of pretreatment 18F-FDG PET in patients with primary central nervous system lymphoma: SUV-based assessment. J Neurooncol 2010;100:225-32.
129. Kasenda B, Haug V, Schorb E, et al. 18F-FDG PET is an independent outcome predictor in primary central nervous system lymphoma. J Nucl Med 2013;54:184-91.
130. Okuyucu K, Alagoz E, Ince S, et al. Can metabolic tumor parameters on primary staging (18)F-FDG PET/CT aid in risk stratification of primary central nervous system lymphomas for patient management as a prognostic model? Rev Esp Med Nucl Imagen Mol 2018;37:9-14.
131. Krebs S, Mellinghoff I, Grommes C, et al. Prognostic value of FDG-PET/CT in recurrent/refractory CNS lymphoma receiving Ibrutinib-based therapies. Eur J Nucl Med Mol Imaging 2019;46:S260-1.</jrn>
132. Lau EW, Drummond KJ, Ware RE, et al. Comparative PET study using F-18 FET and F-18 FDG for the evaluation of patients with suspected brain tumour. J Clin Neurosci 2010;17:43-9.
133. Okada Y, Nihashi T, Fujii M, et al. Differentiation of newly diagnosed glioblastoma multiforme and intracranial diffuse large B-cell lymphoma using (11)C-methionine and (18)F-FDG PET. Clin Nucl Med 2012;37:843-9.
134. Puranik AD, Boon M, Purandare N, et al. Utility of FET-PET in detecting high-grade gliomas presenting with equivocal MR imaging features. World J Nucl Med 2019;18:266-72.
135. Albert NL, Weller M, Suchorska B, et al. Response Assessment in Neuro-Oncology working group and European Association for Neuro-Oncology recommendations for the clinical use of PET imaging in gliomas. Neuro Oncol 2016;18:1199-208.
136. Kawai N, Okubo S, Miyake K, et al. Use of PET in the diagnosis of primary CNS lymphoma in patients with atypical MR findings. Ann Nucl Med 2010;24:335-43.
137. Kawase Y, Yamamoto Y, Kameyama R, et al. Comparison

of 11C-methionine PET and 18F-FDG PET in patients with primary central nervous system lymphoma. Mol Imaging Biol 2011;13:1284-9.
138. Miyakita Y, Ohno M, Takahashi M, et al. Usefulness of carbon-11-labeled methionine positron-emission tomography for assessing the treatment response of primary central nervous system lymphoma. Jpn J Clin Oncol 2020;50:512-8.
139. Ahn SY, Kwon SY, Jung SH, et al. Prognostic significance of interim 11C-methionine PET/CT in primary central nervous system lymphoma. Clin Nucl Med 2018;43:e259-64.
140. Nomura Y, Asano Y, Shinoda J, et al. Characteristics of time-activity curves obtained from dynamic (11) C-methionine PET in common primary brain tumors. J Neurooncol 2018;138:649-58.
141. Ogawa T, Kanno I, Hatazawa J, et al. Methionine PET for follow-up of radiation therapy of primary lymphoma of the brain. Radiographics 1994;14:101-10.
142. Jang SJ, Lee KH, Lee JY, et al. (11)C-methionine PET/CT and MRI of primary central nervous system diffuse large B-cell lymphoma before and after high-dose methotrexate. Clin Nucl Med 2012;37:e241-4.
143. Li LF, Taw BB, Pu JK, et al. Primary Central Nervous System Natural Killer Cell Lymphoma in a Chinese Woman with Atypical (11)C-Choline Positron Emission Tomography and Magnetic Resonance Spectrometry Findings. World Neurosurg 2015;84:1176.e5-9
144. Sasikumar A, Joy A, Pillai MR, et al. Diagnostic value of 68Ga PSMA-11 PET/CT imaging of brain tumors-preliminary analysis. Clin Nucl Med 2017;42:e41-8.
145. Herhaus P, Lipkova J, Lammer F, et al. CXCR4-targeted positron emission tomography imaging of central nervous system B-cell lymphoma. J Nucl Med 2020;61:1765-71.
146. Hovhannisyan N, Fillesoye F, Guillouet S, et al. [(18)F] Fludarabine-PET as a promising tool for differentiating CNS lymphoma and glioblastoma: Comparative analysis with [(18)F]FDG in human xenograft models. Theranostics 2018;8:4563-73.
147. Brunn A, Montesinos-Rongen M, Strack A, et al. Expression pattern and cellular sources of chemokines in primary central nervous system lymphoma. Acta Neuropathol 2007;114:271-6.
148. Montgomery JA, Hewson K, Temple C Jr. Synthesis of potential anticancer agents. (1-aziridinyl)purines. J Med Pharm Chem 1962;5:15-24.
149. Gandhi V, Plunkett W. Cellular and clinical pharmacology of fludarabine. Clin Pharmacokinet 2002;41:93-103.
150. Anderson VR, Perry CM. Fludarabine: a review of its use in non-Hodgkin's lymphoma. Drugs 2007;67:1633-55.
151. Goodman ER, Fiedor PS, Fein S, et al. Fludarabine phosphate: A DNA synthesis inhibitor with potent immunosuppressive activity and minimal clinical toxicity. Am Surg 1996;62:435-42.
152. Guillouet S, Patin D, Tirel O, et al. Fully automated radiosynthesis of 2-[18F]fludarabine for PET imaging of low-grade lymphoma. Mol Imaging Biol 2014;16:28-35.
153. Nguyen AV, Blears EE, Ross E, et al. Machine learning applications for the differentiation of primary central nervous system lymphoma from glioblastoma on imaging: A systematic review and meta-analysis. Neurosurg Focus 2018;45:E5.
154. Alcaide-Leon P, Dufort P, Geraldo AF, et al. Differentiation of enhancing glioma and primary central nervous system lymphoma by texture-based machine learning. AJNR Am J Neuroradiol 2017;38:1145-50.

doi: 10.21037/aol-20-52
Cite this article as: Krebs S, Barasch JG, Young RJ, Grommes C, Schöder H. Positron emission tomography and magnetic resonance imaging in primary central nervous system lymphoma—a narrative review. Ann Lymphoma 2021;5:15.

Supplementary

Table S1 Selected studies reporting utility of FDG PET/CT in diagnosing primary CNS lymphoma

Reference	No.	SUV_{max}	TNR	Comment
Albano (107)	46	15.6±9.2 (range, 5–47)	3.1±1.7* (range, 1.4–10.6)	PCNSL (n=44), SCNSL (n=2)
				Immunocompetent (n=41), immunodeficient (n=5)
				Clearly avid disease (n=38), no distinct avid lesions seen (n=8)
				PET/CT detected extracranial disease (n=2; SCNSL)
Kosaka (121)	34	22.17±5.03 (n=7)	3.29±1.03*	PCNSL (n=7), HGG/brain metastasis (n=27)
				Using an SUV_{max} of 15.0 as a cutoff for diagnosing CNS lymphoma, only one HGG was found as a false-positive (SUV_{max} 18.8)
Kawai (136)	17	13.88±5.46 (n=16)	N/A	Newly diagnosed primary CNS lymphoma (DLBCL) (n=17)
				"Atypical" primary CNS lymphoma (n=5): T1W MRI: disseminated lesions with irregular margin affecting multiple regions of the brain (n=3); no lesion (n=1), ring-like enhancing lesion (n=1); thereof, n=4 analyzed on PET; PET: no distinct avid lesion (n=4); SUV_{max} 8.35±1.69 (n=4)
				"Typical" primary CNS lymphoma (n=12): T1W MRI: single lesion (n=5) or multiple lesions (n=7), total: n=12 patients; PET: clearly avid lesion (n=4); SUV_{max} 15.73±5.01 (n=12)
				Kinetic analysis may be helpful in diagnosis of atypical primary CNS lymphoma
Purandare (122)	101	Median (range): 20.3 (8.1–46.3) (n=25)	N/A	Primary CNS lymphoma (n=21), secondary CNS lymphoma (n=4), GBM (n=30), metastasis (46)
				PET/CT detected extracranial disease (n=4; secondary CNS lymphoma)
				Using a cut-off of SUV_{max} of 15.5 has an 84% sensitivity and 80% specificity to diagnose lymphomas (AUC =0.876, P=0.00)
Zhou (100)	92	17.66±7.37 (n=40)	2.46±1.04**	Primary CNS lymphoma (n=40), GBM (n=52)
				SUV_{max} + TNR may enable reliable differentiating primary CNS lymphoma from GBM [AUC (95% CI): 0.923 (0.854–0.966)]
				PET parameters SUV_{max}, SUV_{mean}, and TLG were inversely proportional to the rADCs of primary CNS lymphoma lesions

*, SUV_{max}(tumor)/SUV_{max}(normal cortical brain); **, SUV_{max}(tumor)/SUV_{mean} (contralateral normal cortical brain). SUV, standardized uptake value; N/A, not available; TNR, tumor to normal contralateral cortex activity ratio; PCNSL, primary central nervous system lymphoma; PET, positron emission tomography; CT, computed tomography; SCNSL, secondary central nervous system lymphoma; HGG, high-grade glioma; CNS, central nervous system; DLBCL, diffuse large B-cell lymphoma; T1W, T1-weighted; MRI, magnetic resonance imaging; GBM, glioblastoma; AUC, area under the curve; rADCs, relative apparent diffusion coefficient.

http://dx.doi.org/10.21037/aol-20-52